

Article

Investigating the Influence of Flue Gas Induced by Coal Spontaneous Combustion on Methane Explosion Risk

Sijia Hu ^{1,2,3}, Yanjun Li ^{1,2,3,*}, Chuanjie Zhu ^{2,3}, Baiquan Lin ^{2,3}, Qingzhao Li ^{2,3}, Baolin Li ^{1,2,3} and Zichao Huang ^{4,*} 

¹ School of Environment and Safety Engineering, North University of China, Taiyuan 030051, China; tb19120011b2@cumt.edu.cn (S.H.); 20220060@nuc.edu.cn (B.L.)

² Key Laboratory of Gas and Fire Control for Coal Mines, Ministry of Education, China University of Mining and Technology, Xuzhou 221116, China; anq021@cumt.edu.cn (C.Z.); lbq21405@126.com (B.L.); qingzhaolee@163.com (Q.L.)

³ School of Safety Engineering, China University of Mining and Technology, Xuzhou 221116, China

⁴ Industrial Safety Research Branch, China Coal Technology and Engineering Group Chongqing Research Institute, Chongqing 400037, China

* Correspondence: 20230116@nuc.edu.cn (Y.L.); passion_hzc@163.com (Z.H.)

Abstract: During the process of coal spontaneous combustion (CSC), a plethora of combustible gases alongside inert gases, such as CO₂, are copiously generated. However, prior investigations have regrettably overlooked the pivotal influence of inert gas production on the propensity for methane explosions during CSC. To investigate the impact of the flue gas environment generated by CSC, containing both combustible and inert gases, on the risk of methane explosion, a high-temperature programmed heating test system for CSC was employed to analyze the generation pattern of flue gas. It was found that CO, CO₂, and CH₄ were continuously generated in large quantities during the process of CSC, which are the main components of CSC flue gas. The effect of the concentration and component ratio (C_{CO_2}/C_{CO}) of the flue gas on the methane explosion limit was tested. It was found that the CSC flue gas led to a decrease in the methane explosion limit, and that the explosion limit range was facilitated at $0 < C_{CO_2}/C_{CO} < 0.543$ and suppressed at $C_{CO_2}/C_{CO} > 0.543$. As the temperature of CSC increases, the risk of methane explosion is initially suppressed. When the coal temperature exceeds 330–410 °C, the explosion risk rapidly expands.

Keywords: coal spontaneous combustion; gas generation; methane explosion; explosion limit; risk assessment



Citation: Hu, S.; Li, Y.; Zhu, C.; Lin, B.; Li, Q.; Li, B.; Huang, Z. Investigating the Influence of Flue Gas Induced by Coal Spontaneous Combustion on Methane Explosion Risk. *Fire* **2024**, *7*, 105. <https://doi.org/10.3390/fire7040105>

Academic Editors: Chuyuan Huang, Haipeng Jiang and Lijuan Liu

Received: 12 February 2024

Revised: 15 March 2024

Accepted: 21 March 2024

Published: 22 March 2024



Copyright: © 2024 by the authors. Licensee MDPI, Basel, Switzerland. This article is an open access article distributed under the terms and conditions of the Creative Commons Attribution (CC BY) license (<https://creativecommons.org/licenses/by/4.0/>).

1. Introduction

Energy stands as the bedrock of human advancement, with coal wielding a significant sway in global energy consumption [1–3]. Throughout the coal mining process, various disaster risks are encountered, among which methane explosions pose the gravest threat, resulting in profound human casualties and extensive property devastation [4–7]. The residual coal left within mining sites, owing to the inherent limitations in extraction techniques, lays the groundwork for the emergence of coal spontaneous combustion (CSC) [8,9]. When the CSC develops to a high temperature sufficient to detonate methane, it is possible to form a serious methane explosion accident [10]. In the genesis of this high-temperature source, copious volumes of mixed flue gas, comprising combustible and inert constituents, are incessantly generated, exerting a tangible influence on methane explosion risks [11–13]. Delving into the generation law of flue gas during coal spontaneous combustion and its consequential impact on methane explosion limits not only enriches our comprehension of the perils posed by methane explosion disasters stemming from coal spontaneous combustion in goaf but also fortifies our arsenal of preventive and mitigation measures against such calamitous events [14,15]. Hence, a plethora of scholarly endeavors have been dedicated to scrutinizing the methane explosion risk under the aegis of CSC conditions [16].

The genesis of combustible gases poses a palpable escalation in the risk profile of methane explosions [17–19]. In a study by Zhang et al., the impact of CO on methane explosion limits was examined across varying temperature regimes, employing a 20 L explosive sphere apparatus. Their findings elucidated a conspicuous augmentation in gas explosion risk concomitant with heightened initial temperatures and CO concentrations [20]. Hao et al. conducted investigations into the influence of H₂ on methane explosion risks, uncovering a notable expansion in the explosion limit range of methane due to the presence of H₂ [19]. Further delving into this intricate nexus, Ma et al. probed the effects of CO-H₂ mixtures on methane explosion limits. Their comprehensive analysis unveiled a discernible decrease in the lower explosion limit (LEL) and a noteworthy expansion in methane explosion limits, thereby substantially amplifying methane explosion risks, with CO-H₂ mixtures demonstrating a more pronounced effect compared to pure CO [14]. Wang et al. undertook experiments centered on the spontaneous combustion gas emissions of long-flame coal to scrutinize the impact of CO-C₂H₄-C₂H₆ mixtures on methane explosion limits. Their discernments highlighted a heightened explosion hazard attributed to the addition of these combustible gases, with C₂H₄ and C₂H₆ exerting more significant effects than CO [21]. Building upon the foundations laid by Wang et al., Luo et al. expanded the purview of inquiry by incorporating the influence of H₂, revealing a parabolic increase in methane explosion hazards within CSC mixtures [22].

While significant strides have been made in scrutinizing the impact of gases engendered during coal spontaneous combustion (CSC) on methane explosion risks, these endeavors are not devoid of certain lacunae. Primarily, extant investigations predominantly center on gas analyses at temperatures below 500 °C [23,24], whereas the temperature required for CSC to ignite methane often needs to exceed 650 °C [25]. Moreover, prevailing studies tend to concentrate on the effects of individual combustible gases or their mixtures generated during CSC on methane risk, neglecting the distinctive characteristic of yielding copious volumes of mixed gas comprising both combustible and inert constituents during coal spontaneous combustion. This oversight inevitably engenders inaccuracies in analysis outcomes [13]. Therefore, in this study, the variation law of the concentration and composition of gases generated during the process of CSC temperature rising to 730 °C was analyzed. The impact of flue gas, characterized by varying concentrations and composition ratios, on methane explosion limits was systematically evaluated, thereby elucidating the dynamics of methane explosion risk under the influence of flue gas in relation to coal temperature.

2. Flue Gas Generation Characteristics during CSC

2.1. The Flue Gas Generation Characteristic Test Experiment of CSC

2.1.1. Experimental System

The temperature-programmed experiment serves as a cornerstone method for elucidating the gas generation law of CSC [26]. Given that CSC-induced methane explosions necessitate attaining temperatures exceeding 600 °C, a high-temperature programmed experimental system was built, as illustrated in Figure 1. The system was composed of a gas supply system, programmed temperature control system, temperature acquisition system, and gas analysis system. The gas supply system consisted of gas cylinders, flow controllers, gas mixing tanks, check valves, and gas purifiers. In order to simulate the air conditions in the goaf of coal mine, O₂ and N₂ were used as the gas source. The input gas flow was meticulously regulated by high-precision gas flow controllers, maintaining an N₂/O₂ ratio of 4. The programmed temperature control system was composed of an SG-GL1400 vacuum tube furnace (heating range 0~1400 °C, maximum heating rate 10 °C/min) and a coal sample container of 316 stainless steel. The coal samples were broken and screened to obtain particles with a size range of 40–80 mesh. Subsequently, these particles were placed into coal sample containers, sealed, and then placed horizontally in a vacuum tube furnace to ensure uniform heating of the coal sample container. The temperature acquisition system was composed of thermocouples and a temperature acquisition instrument. The

measurement accuracy of the thermocouple was $0.1\text{ }^{\circ}\text{C}$. The temperature changes inside the container were collected in real-time. The gases generated during the coal heating process were collected in gas sampling bags and analyzed using a GC-4000A gas chromatograph.

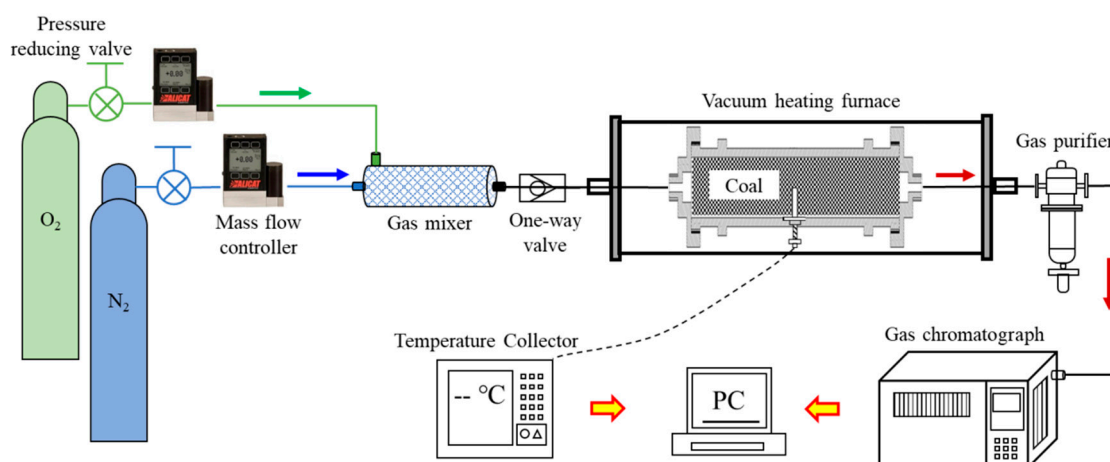


Figure 1. Schematic diagram of high-temperature programmed experiment system.

2.1.2. Experimental Process

- (1) Coal samples screening: The fresh coal samples taken from the site were removed by sandpaper, and then the coal samples were broken into different sizes by a crusher. Then, the coal samples were screened by a sieve with a screening range of 0.18–0.38 mm to obtain a coal sample with a particle size range of 40~80 mesh. Finally, 300 g coal samples were selected and placed in a vacuum-drying oven at $50\text{ }^{\circ}\text{C}$ for 24 h to remove external moisture.
- (2) Heating pretreatment: After the dry coal samples were loaded into the coal sample container, N_2 was first introduced into the furnace at a flow rate of 120 mL/min for about 10 min to drain the air in the tank. Subsequently, the furnace temperature was set at $30\text{ }^{\circ}\text{C}$ and maintained for 30 min to make the initial temperature conditions of the experiment consistent.
- (3) Temperature programming: The flow controller was adjusted to supply gas to the coal sample tank at 300 mL/min , and the proportion of O_2 in the supplied gas was 21%. At the same time, the flow and composition of the outlet gas were monitored. After the outlet gas was stable, the programmed temperature control system was turned on, and the heating rate was set to $2\text{ }^{\circ}\text{C/min}$, and the heating range was $30\text{--}710\text{ }^{\circ}\text{C}$.
- (4) Data collecting: After the temperature started to rise, the temperature acquisition instrument was opened, and the acquisition frequency was set to 1 time/s. At the same time, for every $20\text{ }^{\circ}\text{C}$ increase in coal temperature, flue gas generated from coal spontaneous combustion was collected and stored separately in gas bags with a volume of 10 mL each. Subsequently, the flue gas in each gas bag was tested using the chromatograph.

2.1.3. Experimental Samples

Three types of coal samples with different degrees of metamorphism were selected for testing to analyze the generation law of combustible and inert gases during the CSC process. These coal samples were obtained from the Shengli Coal Mine in the Inner Mongolia Autonomous Region (lignite), Baikuang Coal Mine in Pingdingshan, Henan Province (bituminous coal), and the Linhua Coal Mine in Guizhou Province (anthracite). The industrial analysis and vitrinite reflectance test results of the coal samples are shown in Table 1.

Table 1. Reflectance and industrial analysis of coal sample maceral groups.

Coal Samples	Proximate Analysis (<i>w/w</i> %)				Vitrinite Reflectance $R_{0, \max}$ (%)
	M_{ad}	A_{ad}	V_{daf}	FC_{ad}	
Lignite	11.37	14.63	53.41	20.59	0.32
Bituminous	1.16	9.37	24.60	64.87	1.22
Anthracite	2.18	15.45	6.64	75.73	3.33

2.2. Flue Gas Generation Law of CSC

Figure 2 portrays the dynamic interplay between gas concentrations and coal temperature throughout the heating process. Across the spectrum of temperatures spanning from 30 to 710 °C, the gases emanating from the heating of three distinct coal types predominantly encompass CO, CO₂, CH₄, C₂H₄, C₂H₆, and C₃H₈. The initial concentrations of CO and CO₂ for lignite, bituminous coal, and anthracite were 0.0029% and 0.27%, 0.0022% and 0.22%, and 0.0017% and 0.16%, respectively. Notably, the emergence of CO and CO₂ pervaded the entirety of the coal’s thermal evolution, steadfastly constituting the principal constituents of the generated gases. The advent of CH₄ burgeoned notably once the coal temperature surpassed the threshold of 290 °C, exhibiting a sustained propensity for generation even amidst the heightened temperatures. This phenomenon underscores the potential for localized explosion hazards in regions with diminished methane content in the goaf, where evaluation in coal temperature can instigate methane release. In contrast, the generation of C₂H₄, C₂H₆, and C₃H₈ predominates within the temperature band of 350 to 550 °C, yielding relatively diminutive quantities, each remaining below 0.5. Consequently, the influence of these gases on methane explosions remains circumscribed. Thus, in instances of (CSC) within the goaf, the gases prone to amass in the combustion zone primarily comprise CO, CO₂, and CH₄. Among them, CH₄ is the inherent gas in the goaf, while CO and CO₂, as gases generated in large quantities during the coal heating process, may affect methane explosions. Accordingly, this investigation delves into the ramifications of CSC flue gas, predominantly constituted by CO and CO₂, on the risk of methane explosions.

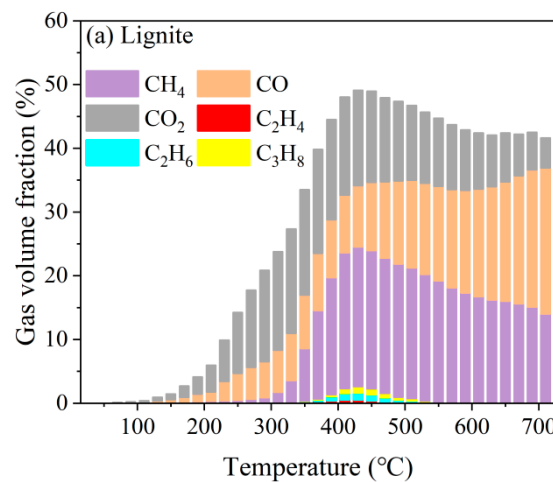


Figure 2. Cont.

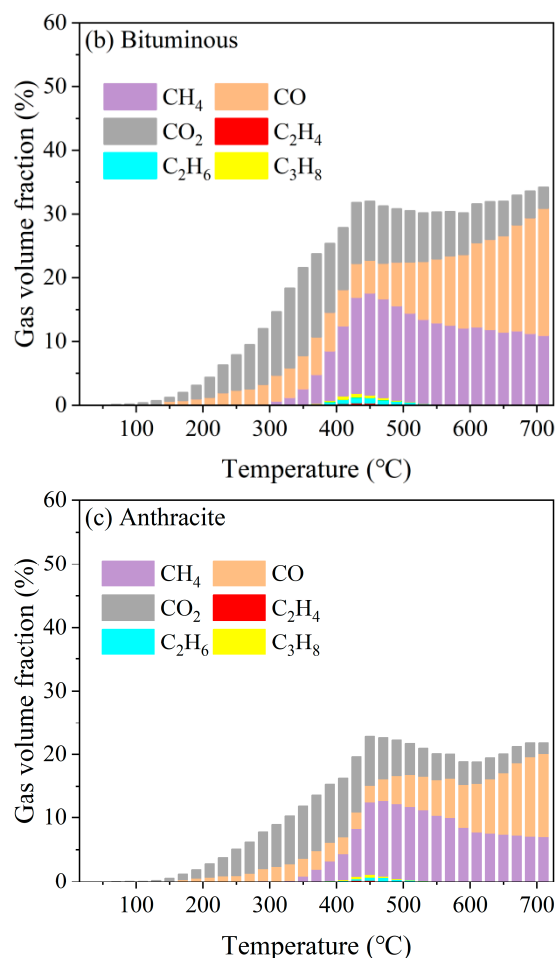


Figure 2. Generation law of CSC flue gas.

3. Influence of CSC Flue Gas on Methane Explosion Limit

The determination of the explosion limits of combustible gases was achievable through both experimental and theoretical calculation methodologies [27,28]. Despite the array of theoretical approaches available for calculating these limits, experimental validation remains the gold standard [22,29,30]. Consequently, this study endeavored to employ experimental testing as the cornerstone for investigating the explosion limits of methane in the presence of flue gas.

3.1. Explosion Limit Test Experiment of Multi-Component Mixed Gas

3.1.1. Experimental System

In order to investigate the effect of CSC flue gas on the explosion limits of methane, a multi-component gas explosion limit testing experimental system was constructed as shown in Figure 3, mainly composed of an explosion room, gas supply system, ignition system, and data acquisition system. The explosion room was a cylindrical chamber made of 304 stainless steel, with a volume of 16 L and was capable of withstanding an explosion pressure of 10 MPa. The gas supply system mainly consisted of gas cylinders, control valves, driers, vacuum pumps, and high-precision vacuum gauges. The gas was supplied using Dalton's law of partial pressures. During the supply process, precise control of gas concentration as achieved through a high-precision vacuum gauge, with an accuracy of up to 0.01%. The ignition system consisted of ignition electrodes and an ignition controller, with a gap of 2 mm between the positive and negative electrodes. The ignition controller was a KTD-W adjustable igniter capable of releasing ignition energy ranging from 50 to 500 mJ. The data acquisition system consisted of a high-frequency pressure sensor

and a TST6300 dynamic signal acquisition instrument. The highest sampling frequency for explosion overpressure was 1 MHz, with a maximum sampling width of 2 M and a sampling accuracy of up to ± 0.001 FS. According to the European Union standard BSEN 1839:2012, the criterion for an explosion is whether the maximum explosion pressure exceeds 5% of the initial pressure [31].

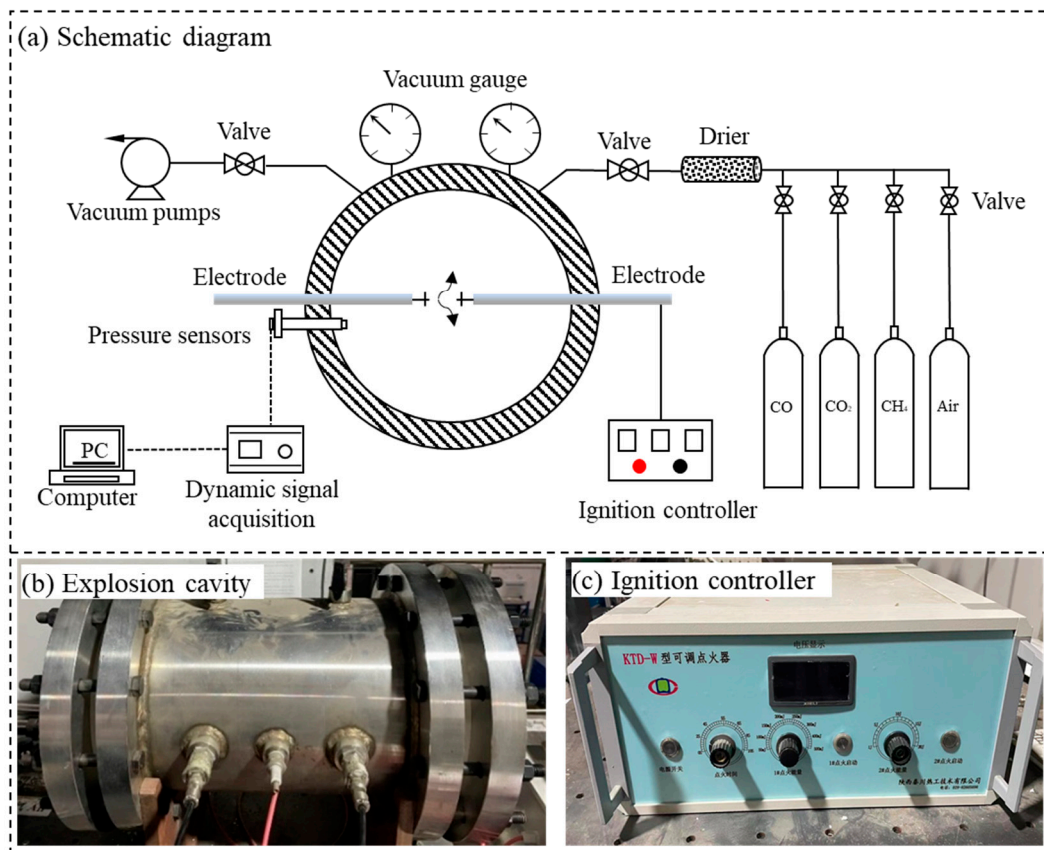


Figure 3. Experimental system for testing the explosion characteristics of multi-component gases.

3.1.2. Experimental Process

- (1) **Experimental preparation:** Before the experiment, the line connections and the air tightness of the device were checked separately. The ignition system and explosion overpressure acquisition system were debugged under unpressurized conditions to ensure the normal operation of the testing apparatus.
- (2) **Vacuuming:** The intake valve was closed, the vacuum pump was turned on, the high-precision vacuum pressure gauge was observed, and once the pressure decreased to a stable level, the vacuuming valve was closed.
- (3) **Gas supply:** The partial pressure of each gas according to Dalton's law was calculated, then sequentially the gas valve was opened and the concentration of each gas was controlled using the vacuum pressure gauge. After completion, the gases were allowed to stand for 10 min to ensure thorough mixing.
- (4) **Ignition:** The explosion overpressure signal acquisition was turned on, then the mixed gas was ignited using the igniter controller.
- (5) **Exhaust the waste gas:** After the explosion ended, the exhaust valve was opened and dry air was introduced into the explosion room via the intake pipe for 30 s to purge any remaining explosive gases inside the chamber.

3.1.3. Experimental Design

In accordance with the generation law of CSC flue gas, CO and CO₂ emerged as prominent constituents capable of sustained and copious generation, each bearing distinct implications for methane explosion limits [32–34]. Therefore, this study took the concentration of flue gas (C_{flue}) and the concentration ratio of CO₂ to CO in flue gas (α) as influencing factors to analyze the influence of CSC flue gas on the methane explosion limit. To analyze the variation trends of C_{flue} and α with coal temperature, corresponding values of C_{flue} and α were calculated based on the CO and CO₂ concentrations obtained at each temperature adjustment as depicted in the experimental results of Figure 2. The results are presented in Figure 4. From Figure 4a, it is discernible that during the initial phases of coal temperature elevation, the concentration of flue gas remains relatively modest, with none of the three coal samples surpassing 1%. Subsequently, upon attaining 150 °C, the rate of flue gas generation escalates swiftly, albeit not exceeding 30% at its zenith. Figure 4b delineates the rapid initial decline followed by a gradual stabilization of α as coal temperature escalates. Prior to reaching 150 °C, the flue gas concentration remains relatively subdued, exerting limited impact on methane explosion limits. Consequently, this study directs its focus towards scrutinizing the effect of CSC flue gas on methane explosion limits subsequent to coal temperature surpassing 150 °C. During this phase, the α value of the flue gas predominantly oscillates within the range of 0 to 5.

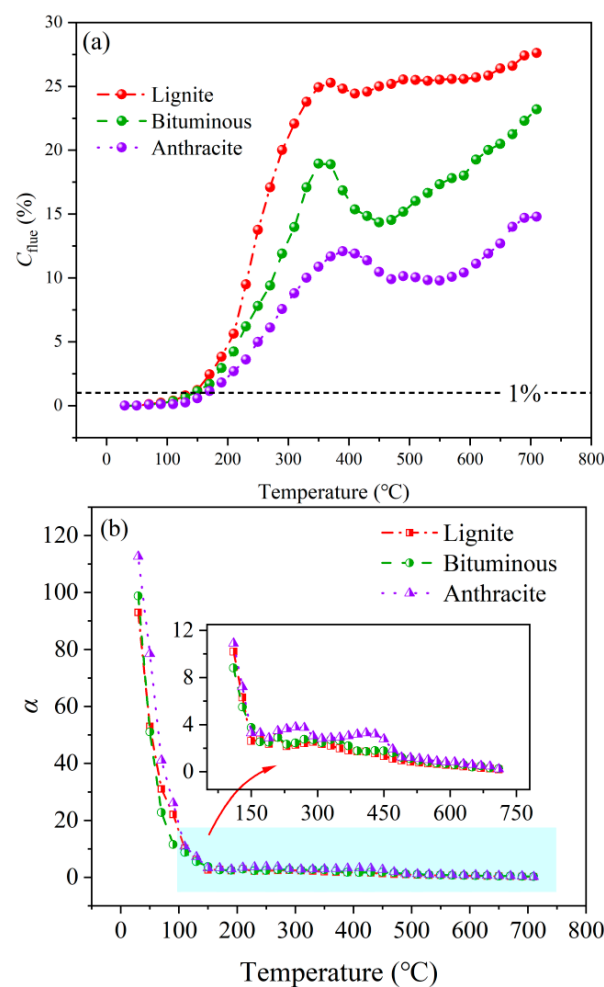


Figure 4. Variations of C_{flue} and α with the increase in coal temperature.

Based on the preceding analysis, the concentration of flue gas generated by CSC predominantly fluctuates between 1% and 30%, while the α value primarily ranges from 0 to 5. In light of this, to scrutinize the impact of flue gas on methane explosion limits, six distinct concentration conditions of flue gas were devised, namely 5%, 10%, 15%, 20%, 25%, and 30%. Additionally, 5 α value conditions were delineated, encompassing 0.2, 0.5, 1, 3, and 5.

3.2. Experiments

Figure 5 delineates the repercussions of CSC flue gas, characterized by varying concentrations (C_{flue}) and α values, on methane explosion limits. Notably, the presence of CSC flue gas precipitates a decline in both the lower explosion limit (LEL) and upper explosion limit (UEL) of methane. This trend is similar to the experimental findings in reference [35], but the values are slightly higher than the test values in reference [35]. This may be due to different explosion limit standards and experimental conditions. The reduction in UEL is ascribed to the competitive influences of CO and CO₂ on O₂ molecules, coupled with the dilution, insulation, and cooling effects of CO₂ on reactants, alongside the inhibitory impact of CO₂ on the reaction process. Furthermore, as the proportion of CO₂ in the flue gas mixture escalates, the role of CO₂ becomes more conspicuous, yielding a more pronounced decrease in the UEL. However, the reasons for the decline of LEL are different from those of UEL. CO tends to diminish the LEL of methane, whereas CO₂ tends to elevate it. The reason for the decrease in LEL of methane is that the effect of CO in the flue gas ($\alpha = 0\sim 5$) is stronger than that of CO₂. Consequently, while the decrease in LEL may engender fresh explosion hazards in regions where methane concentrations were initially sub-threshold, the continuous escalation of C_{flue} , particularly in scenarios such as $\alpha = 0.2$, can drive the LEL of methane to 0%, rendering the flue gas itself explosively susceptible, thereby heightening the likelihood of ignition or explosion.

The effects of different flue gases with varying C_{flue} or α on the methane explosion limits are different. When α remains constant, both the LEL and UEL of methane decrease linearly with the increase in C_{flue} . However, when C_{flue} remains constant, the impact of flue gases with different α on the UEL and LEL of methane varies. Specifically, the UEL decreases with increasing α , while the LEL increases with increasing α .

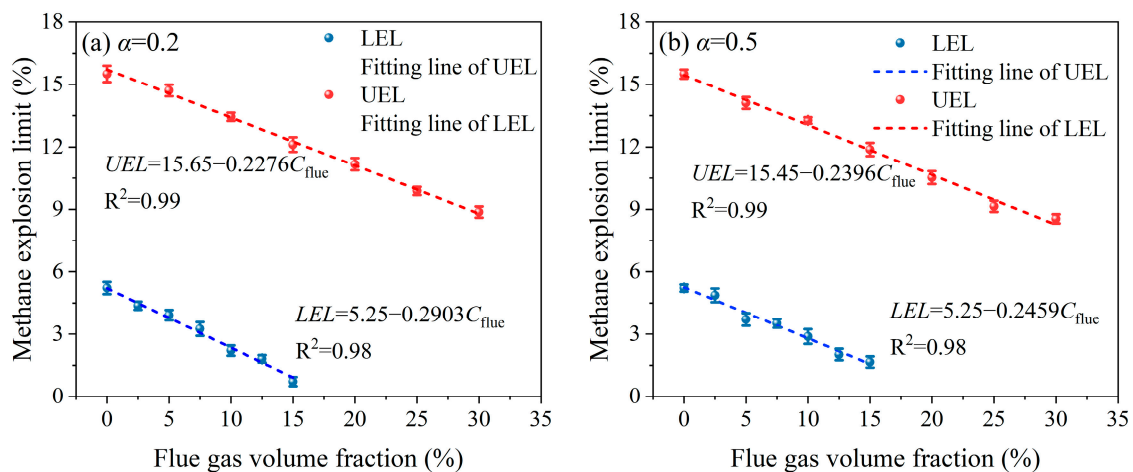


Figure 5. Cont.

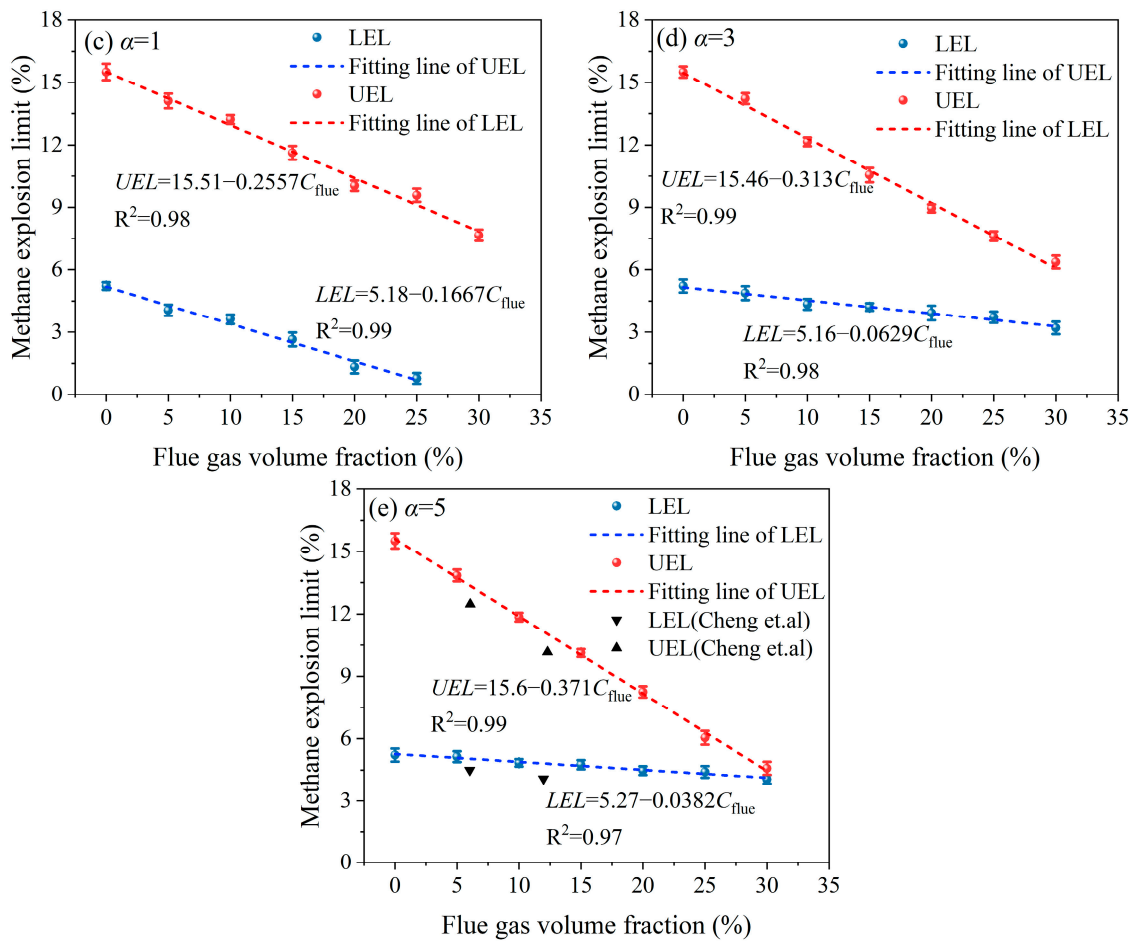


Figure 5. Influence of flue gases of different C_{flue} and α on the methane explosion limit [35].

4. Influence of CSC Flue Gas on the Risk of Methane Explosion

4.1. Influence of Flue Gas on Methane Explosion Limit Range

The explosion limit range stands as a pivotal parameter for assessing explosion risks [36,37]. In the context of this study, the measured methane explosion limit spans from 5.22% to 15.51%, yielding a range of 10.29%. Figure 6 elucidates the impact of flue gas characterized by diverse C_{flue} and α values on the range of methane explosion limits. It is discernible that flue gas with varying α values exerts disparate effects on the explosion limit range of methane. Specifically, when α assumes values of 0.2 or 0.5, the flue gas augments the explosion limit range of methane. Notably, when $C_{flue} \geq 25\%$, there appears to be a decline in the explosion limit range of methane. However, this decline does not signify a mitigation of methane explosion risks. Rather, it signals that flue gas at elevated concentrations possesses explosive characteristics, thereby posing a heightened risk of direct ignition. Conversely, when α is 1, 3, or 5, the flue gas manifests an inhibitory effect on the explosion limit range of methane. Moreover, this inhibitory influence amplifies with escalating C_{flue} .

The fluctuations in the range of methane explosion limits are intricately influenced by both LEL and UEL. Specifically, when the LEL of methane exhibits a slower decline with increasing C_{flue} compared to the UEL, the range of the gas explosion limit contracts. When the decrease rate of the methane LEL with increasing C_{flue} is faster than that of UEL, the explosion limit range of methane expands. Conversely, if the rate of decrease in the methane LEL with increasing C_{flue} surpasses that of the UEL, the explosion limit range of methane expands.

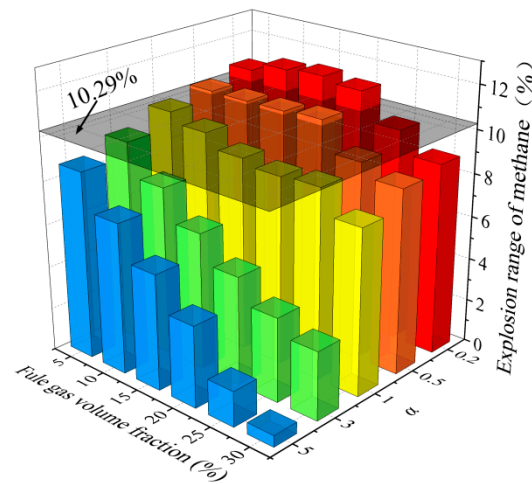


Figure 6. Influence of flue gas on the explosion range of methane.

This rate of decrease can be quantified by the absolute value of the slope ($|k|$) of the linear reduction in the methane explosion limit. In essence, when $|k|_{LEL} > |k|_{UEL}$, flue gas augments the explosion limit range of methane. Conversely, when $|k|_{LEL} < |k|_{UEL}$, flue gas constrains the explosion limit range of methane.

As illustrated in Figure 7, the variation of $|k|$ with α is delineated. It can be observed that $|k|_{LEL}$ decreases as α increases, while $|k|_{UEL}$ increases with α . Notably, at $\alpha = 0.543$, $|k|_{LEL} = |k|_{UEL}$, signifying a point where the impact of flue gas on both the UEL and LEL of methane is equivalent. Consequently, the methane explosion limit range is consistent with the condition without flue gas. In other words, the value of 0.543 denotes the critical threshold at which flue gas transitions from promoting to inhibiting the methane explosion limit range.

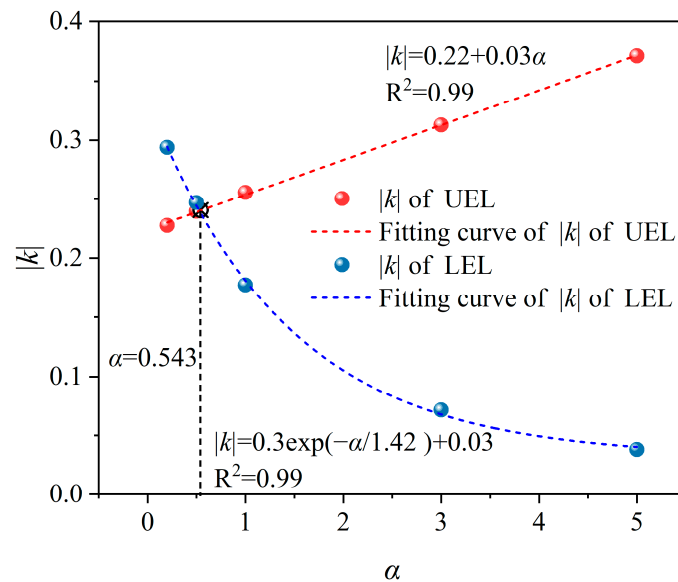


Figure 7. The variation law of $|k|$ with α .

In summation, flue gas characterized by low α values tends to enhance the explosion limit range of methane, whereas flue gas with high α values tends to curtail it. Considering the actual conditions in coal mine goafs, C_{flue} remains relatively subdued during the initial stages of temperature elevation, thereby exerting minimal influence on the explosion limit range of methane. However, as the coal temperature continues to rise, C_{flue} steadily escalates while α gradually diminishes, signaling a trajectory of heightened methane

explosion risk. Particularly during the high-temperature phases, when the α of flue gas plummets below 0.5, the flue gas itself acquires explosive properties, precipitating a sudden upsurge in the risk of explosion within the goaf area.

4.2. Variation Law of Methane Explosion Risk during the Temperature Increasing Process of CSC

4.2.1. Fitting of Methane Explosion Limits under the Influence of Flue Gas

The elevated temperatures generated by CSC in the goaf serve as crucial ignition sources for initiating methane combustion [38,39]. Concurrently, flue gas undergoes continuous generation throughout the coal temperature escalation process within the goaf, culminating in the formation of a dynamic flue gas environment characterized by fluctuating C_{flue} and α values. This, in turn, exerts a notable influence on the explosion limits of methane.

To assess the risk of methane explosion amidst coal temperature elevation, the methane explosion limit within the flue gas milieu was modeled. as shown in Figure 8. The specific outcomes of this fitting process are as follows:

$$LEL = 5.22 - 0.3C_{flue}EXP(-\alpha/1.42) - 0.03C_{flue} \tag{1}$$

$$UEL = 15.52 - 0.22C_{flue} - 0.03\alpha C_{flue} \tag{2}$$

where LEL is the lower explosion limit of methane, %; UEL is the upper explosion limit of methane, %; C_{flue} is the flue gas concentration, %; and α is the ratio of CO_2 and CO concentrations in the flue gas.

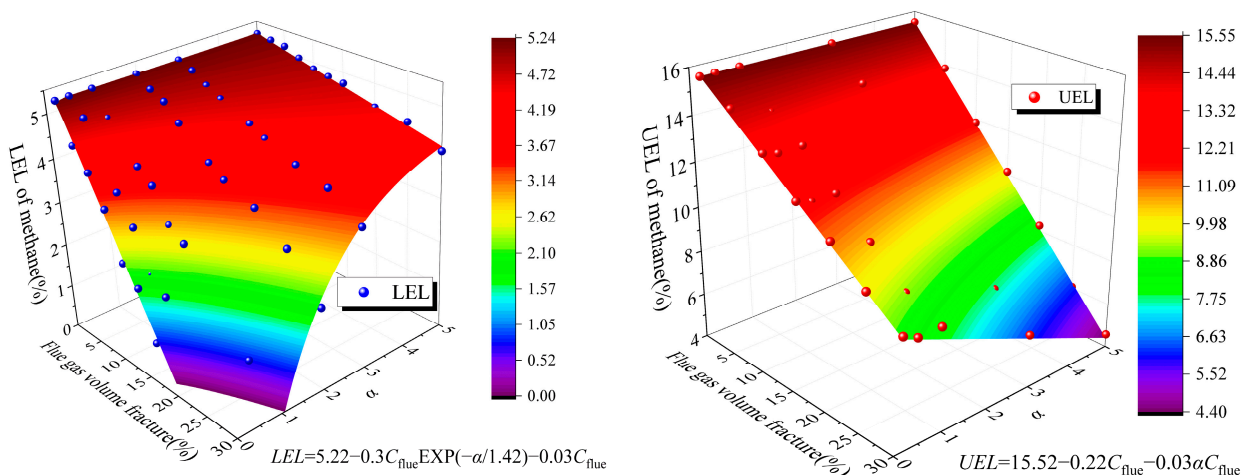


Figure 8. Methane explosion limit fitting.

4.2.2. Variation Law of Methane Explosion Limits during the Temperature Increasing Process of CSC

To assess the explosion risk of methane during the process of coal temperature elevation, it is necessary to calculate the methane explosion limits at various temperatures. By substituting the experimental results of the temperature-programmed experiment into the aforementioned fitted formula for explosion limits calculation, the variation pattern of methane explosion limits with coal temperature was obtained, as depicted in Figure 9. Notably, from the pattern of LEL variation illustrated in Figure 9a, it becomes apparent that under the influence of flue gas, the LEL of methane undergoes a continuous decline with increasing coal temperature. In the oxidation zone of the goaf, the methane concentration typically remains at a low level owing to air dilution, thereby mitigating methane explosion risks [40,41]. However, the presence of flue gas serves to diminish the LEL of methane, thereby introducing new explosion hazards in areas that were initially non-explosive. Something that is particularly noteworthy is the scenario wherein the temperature of bituminous and anthracite coal reaches 550 °C and 650 °C, respectively, resulting in the LEL of methane

plummeting to 0%. At this juncture, the risk of methane explosion escalates significantly due to the combustibility of the flue gas itself.

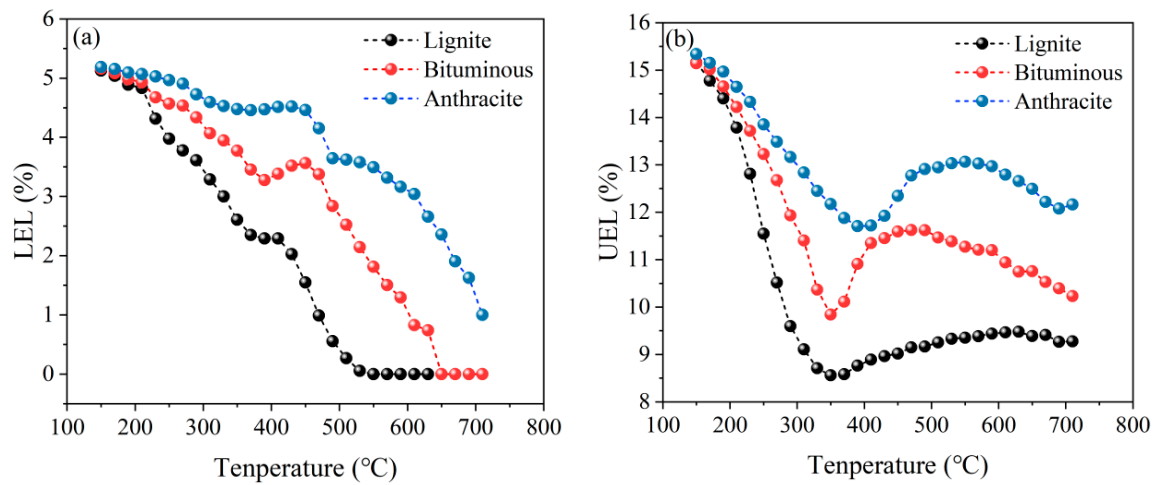


Figure 9. Variation law of methane explosion limit during the temperature rising process of coal.

Similarly, Figure 9b shows that the UEL of methane experiences a decrease under the influence of flue gas. However, unlike the pattern observed in LEL variation, fluctuations in UEL emerge after the temperatures of lignite, bituminous coal, and anthracite reach 350 °C, 350 °C, and 390 °C, respectively. In the event of a CSC disaster in the goaf, the reduction in LEL can potentially mitigate the risk of methane explosion. However, this inhibitory effect is constrained by the low methane concentration prevalent in the oxidation zone. Furthermore, it is noteworthy that the impact of flue gas generated by different coal types on the methane explosion limits varies. Lignite exerts the greatest influence, followed by bituminous coal, with anthracite exerting the least impact. This observation implies that the CSC flue gas generated by low metamorphic grade coal is more likely to escalate the risk of methane explosion.

4.2.3. Variation Law of Methane Explosion Limits Range during the Temperature Increasing Process of CSC

In order to further analyze the impact of flue gas on methane explosion risk during the coal temperature elevation process, it is necessary to analyze the variation of methane explosion limit range with coal temperature. This value can be calculated based on the difference between the LEL and the UEL in Figure 9. The results are illustrated in Figure 10. Notably, it becomes evident that as coal temperature rises, the range of methane explosion limits initially diminishes before rebounding. Relative to conditions devoid of flue gas, the presence of flue gas engenders a reduction in the range of methane explosion limits, reaching a nadir when the temperatures of lignite, bituminous coal, and anthracite reach 330 °C, 350 °C, and 410 °C, respectively. At this juncture, although the decrease in methane LEL remains relatively modest, the inhibitory effect on the explosion limit range peaks, thereby yielding the lowest risk of methane explosion. Subsequently, with the swift expansion of the methane explosion limit range and the continual decline in LEL, the risk of methane explosion progressively escalates.

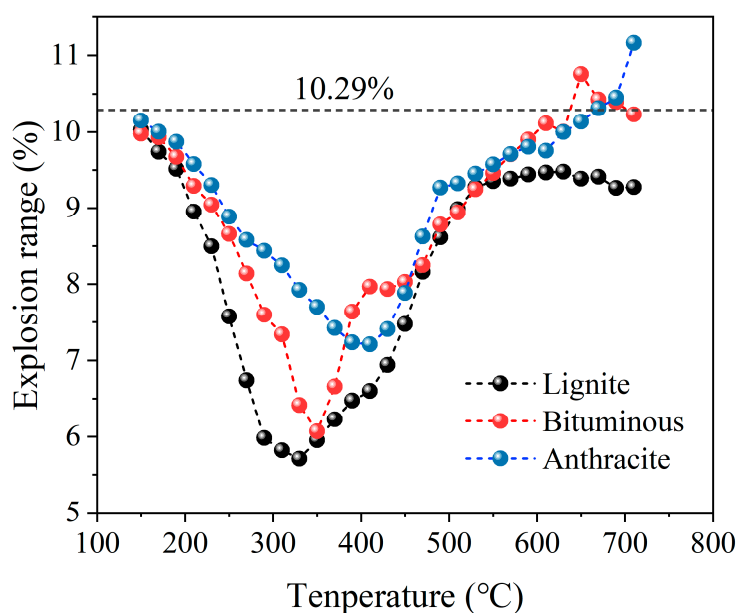


Figure 10. The variation law of methane explosion range during the temperature rising process of coal.

5. Conclusions

- (1) Throughout the CSC temperature elevation process, CO, CO₂, and CH₄ are consistently generated in substantial quantities, constituting the primary components of CSC flue gas. They represent the predominant gases that influence the risk of methane explosions. Conversely, C₂H₄, C₂H₆, and C₃H₈ are produced only in minor quantities within the temperature range of 350~550 °C, and their impact on the risk of methane explosions remains limited.
- (2) Both the LEL and UEL of methane demonstrate a linear decline with increasing C_{flue}. The UEL of explosion diminishes with escalating α , whereas the LEL increases with α .
- (3) Flue gas characterized by lower α values facilitates an expansion of the range of methane explosion limits, whereas flue gas with higher α values constrains the range of methane explosion limits. $\alpha = 0.543$ marks the critical threshold at which flue gas transitions from promoting to inhibiting the explosion limit range of methane.
- (4) At lower coal temperatures, the influence of flue gas on methane LEL is minimal, while the explosion range is inhibited, culminating in a reduced risk of methane explosion. However, once the coal temperature surpasses 330~410 °C, the risk of methane explosion continues to escalate under the dual effects of a rapid decline in LEL and a continuous increase in the explosion limit range.

Author Contributions: Conceptualization, C.Z. and Y.L.; methodology, B.L. (Baiquan Lin); formal analysis, S.H.; investigation, Z.H.; resources, Q.L.; data curation, Y.L.; writing—original draft preparation, S.H.; writing—review and editing, Y.L.; visualization, C.Z.; supervision, Q.L.; project administration, B.L. (Baolin Li); funding acquisition, Y.L. All authors have read and agreed to the published version of the manuscript.

Funding: This research was funded by the National Science and Technology Major Project grant number 2020YFA0711803, the National Natural Science Foundation of China grant number 52174214, 52304260, and Shanxi Province Basic Research Program grant number 202203021222031. And The APC was funded by 202203021222031.

Data Availability Statement: The data in this article is presented in the text and no additional database is required.

Conflicts of Interest: The authors declare no conflict of interest.

References

1. Alshehry, A.; Belloumi, M. The Symmetric and Asymmetric Impacts of Energy Consumption and Economic Growth on Environmental Sustainability. *Sustainability* **2024**, *16*, 205. [\[CrossRef\]](#)
2. Fouquet, R. The Digitalisation, Dematerialisation and Decarbonisation of the Global Economy in Historical Perspective: The Relationship Between Energy and Information Since 1850. *Environ. Res. Lett.* **2024**, *19*, 014043. [\[CrossRef\]](#)
3. Wang, X.; Lu, Y.; Chen, C.; Yi, X.; Cui, H. Total-factor Energy Efficiency of Ten Major Global Energy-consuming Countries. *J. Environ. Sci.* **2024**, *137*, 41–52. [\[CrossRef\]](#)
4. Zhang, X.; Jian, S.; Lin, B.; Zhu, C. Study on the Influence of Different-voltage Plasma Breakdowns on Functional Group Structures in Coal. *Energy* **2023**, *284*, 128768. [\[CrossRef\]](#)
5. Liu, T.; Li, M.; Zou, Q.; Li, J.; Lin, M.; Lin, B. Crack Instability in Deep Coal Seam Induced By the Coupling of Mining Unloading and Gas Driving and Transformation of Failure Mode. *Int. J. Rock Mech. Min. Sci.* **2023**, *170*, 105526. [\[CrossRef\]](#)
6. Li, B.; Wang, E.; Li, Z.; Cao, X.; Liu, X.; Zhang, M. Automatic Recognition of Effective and Interference Signals Based on Machine Learning: A Case Study of Acoustic Emission and Electromagnetic Radiation. *Int. J. Rock Mech. Min. Sci.* **2023**, *170*, 105505. [\[CrossRef\]](#)
7. Zheng, Y.; Li, S.; Xue, S.; Jiang, B.; Ren, B.; Zhao, Y. Study on the Evolution Characteristics of Coal Spontaneous Combustion and Gas Coupling Disaster Region in Goaf. *Fuel* **2023**, *349*, 128505. [\[CrossRef\]](#)
8. Duan, H.; Zhao, L.; Yang, H.; Zhang, Y.; Xia, H. Development of 3D Top Coal Caving Angle Model for Fully Mechanized Extra-thick Coal Seam Mining. *Int. J. Min. Sci. Technol.* **2022**, *32*, 1145–1152. [\[CrossRef\]](#)
9. Liu, Q.; Lin, B.; Zhou, Y.; Li, Y. Permeability and Inertial Resistance Coefficient Correction Model of Broken Rocks in Coal Mine Goaf. *Powder Technol.* **2021**, *384*, 247–257. [\[CrossRef\]](#)
10. Zheng, Y.; Li, Q.; Zhu, P.; Li, X.; Zhang, G.; Ma, X.; Zhao, Y. Study on Multi-field Evolution and Influencing Factors of Coal Spontaneous Combustion in Goaf. *Combust. Sci. Technol.* **2023**, *195*, 247–264. [\[CrossRef\]](#)
11. Ma, D.; Qin, B.; Li, L.; Gao, A.; Gao, Y. Study on the Methane Explosion Regions Induced By Spontaneous Combustion of Coal in Longwall Gobs Using a Scaled-down Experiment Set-up. *Fuel* **2019**, *254*, 115547. [\[CrossRef\]](#)
12. Gao, A.; Qin, B.; Zhang, L.; Ma, D.; Li, L. Experimental Study on Gas Migration Laws at Return Air Side of Goaf Under High-temperature Conditions. *Combust. Sci. Technol.* **2023**, *195*, 1930–1944. [\[CrossRef\]](#)
13. Bai, G.; Li, X.; Zhou, X.; Wang, J.; Linghu, J. Evaluation of Lignite Combustion Characteristics and Gas Explosion Risks Under Different Air Volumes. *Energy Sources Part A Recovery Util. Environ. Eff.* **2020**, *1–15*, 1770375. [\[CrossRef\]](#)
14. Ma, D.; Qin, B.; Zhong, X.; Sheng, P.; Yin, C. Effect of Flammable Gases Produced From Spontaneous Smoldering Combustion of Coal on Methane Explosion in Coal Mines. *Energy* **2023**, *279*, 128125. [\[CrossRef\]](#)
15. Zhuo, H.; Qin, B.; Qin, Q. The Impact of Surface Air Leakage on Coal Spontaneous Combustion Hazardous Zone in Gob of Shallow Coal Seams: A Case Study of Bulianta Mine, China. *Fuel* **2021**, *295*, 120636. [\[CrossRef\]](#)
16. Li, J.; Li, X.; Liu, C.; Zhang, N. Study on the Air Leakage Characteristics of a Goaf in a Shallow Coal Seam and Spontaneous Combustion Prevention and Control Strategies for Residual Coal. *PLoS ONE* **2022**, *17*, e0269822.
17. Yang, Y.; Fei, J.; Luo, Z.; Wen, H.; Wang, H. Experimental Study on Characteristic Temperature of Coal Spontaneous Combustion. *J. Therm. Anal. Calorim.* **2023**, *148*, 10011–10019. [\[CrossRef\]](#)
18. Wang, Y.; Sun, Y.; Dai, L.; Wang, K.; Cheng, G. Mechanisms of CO and CO₂ Production During the Low-temperature Oxidation of Coal: Molecular Simulations and Experimental Research. *Fire* **2023**, *6*, 475. [\[CrossRef\]](#)
19. Hao, Q.; Luo, Z.; Wang, T.; Xie, C.; Zhang, S.; Bi, M.; Deng, J. The Flammability Limits and Explosion Behaviours of Hydrogen-enriched Methane-air Mixtures. *Exp. Therm. Fluid Sci.* **2021**, *126*, 110395. [\[CrossRef\]](#)
20. Zhang, X.; Zhou, X.; Bai, G.; Li, C. Influence of CO on Explosion Limits and Characteristics of the CH₄/air Mixture. *ACS Omega* **2022**, *7*, 24766–24776. [\[CrossRef\]](#)
21. Wang, H.; Liu, Y.; Shan, Q. Influence of Gas From Long-flame Coal Spontaneous Combustion on Gas Explosion Limit. *Int. J. Chem. Eng.* **2023**, *2023*, 5096109. [\[CrossRef\]](#)
22. Luo, Z.; Liang, H.; Wang, T.; Cheng, F.; Su, B.; Liu, L.; Liu, B. Evaluating the Effect of Multiple Flammable Gases on the Flammability Limit of CH₄: Experimental Study and Theoretical Calculation. *Process Saf. Environ. Prot.* **2021**, *146*, 369–376. [\[CrossRef\]](#)
23. Li, H.; Chen, X.; Shu, C.M.; Wang, Q.; Ma, T.; Bin, L. Effects of Oxygen Concentration on the Macroscopic Characteristic Indexes of High-temperature Oxidation of Coal. *J. Energy Inst.* **2019**, *92*, 554–566. [\[CrossRef\]](#)
24. Zhao, J.; Wang, T.; Deng, J.; Shu, C.M.; Zeng, Q.; Guo, T.; Zhang, Y. Microcharacteristic Analysis of CH₄ Emissions Under Different Conditions During Coal Spontaneous Combustion with High-temperature Oxidation and in Situ Ftir. *Energy* **2020**, *209*, 118494. [\[CrossRef\]](#)
25. Robinson, C.; Smith, D.B. The Auto-ignition Temperature of Methane. *J. Hazard. Mater.* **1984**, *8*, 199–203. [\[CrossRef\]](#)
26. Wang, K. An Approach for Evaluation of Grading Forecasting Index of Coal Spontaneous Combustion By Temperature-programmed Analysis. *Environ. Sci. Pollut. Res.* **2023**, *30*, 3970–3979. [\[CrossRef\]](#) [\[PubMed\]](#)
27. Ji, W.; Wang, Y.; Yang, J.; He, J.; Wen, X. Methods to Predict Variations of Lower Explosion Limit Associated with Hybrid Mixtures of Flammable Gas and Dust. *Fuel* **2022**, *310*, 122138. [\[CrossRef\]](#)
28. Wang, G.; Shi, G.; Yang, Y.; Liu, S. Experimental Study on the Exogenous Fire Evolution and Flue Gas Migration During the Fire Zone Sealing Period of the Coal Mining Face. *Fuel* **2022**, *320*, 123879. [\[CrossRef\]](#)

29. Nie, B.; Peng, C.; Gong, J.; Yin, F.; Wang, K. Explosion Characteristics and Energy Utilisation of Coal Mine Ultra-lean Methane. *Combust. Theory Model.* **2021**, *25*, 73–95. [[CrossRef](#)]
30. Jiao, F.; Zhang, H.; Li, W.; Zhao, Y.; Guo, J.; Zhang, X.; Zhang, Y. Experimental and Numerical Study of the Influence of Initial Temperature on Explosion Limits and Explosion Process of Syngas-air Mixtures. *Int. J. Hydrogen Energy* **2022**, *47*, 22261–22272. [[CrossRef](#)]
31. European Committee for Standardisation. *Determination of Explosion Limits of Gases and Vapours: BS EN 1839:2012 [S]*; BIS Standards Publication: Brussels, Belgium, 2012; p. 7.
32. Zhu, X.; Zhou, J.; Guo, Z.; Zhang, X. CO₂ Suppression of Methane/air Explosion Flame and Pressure Coupling Analysis. *Fresenius Environ. Bull.* **2022**, *31*, 4995–5003.
33. Luo, Z.; Su, Y.; Li, R.; Chen, X.; Wang, T. Effect of Inert Gas CO₂ on Deflagration Pressure of CH₄/CO. *ACS Omega* **2020**, *5*, 23002–23008. [[CrossRef](#)] [[PubMed](#)]
34. Deng, J.; Cheng, F.; Song, Y.; Luo, Z.; Zhang, Y. Experimental and Simulation Studies on the Influence of Carbon Monoxide on Explosion Characteristics of Methane. *J. Loss Prev. Process Ind.* **2015**, *36*, 45–53. [[CrossRef](#)]
35. Cheng, F.; Deng, J. Experimental study on the influence of carbon monoxide on carbon dioxide-inerted methane explosion. *Xian Univ. Sci. Technol.* **2016**, *36*, 315–319.
36. Wang, T.; Zhou, Y.; Luo, Z.; Wen, H.; Zhao, J.; Su, B.; Deng, J. Flammability Limit Behavior of Methane with the Addition of Gaseous Fuel at Various Relative Humidities. *Process Saf. Environ. Prot.* **2020**, *140*, 178–189. [[CrossRef](#)]
37. Sun, Y.; Qian, X.; Yuan, M.; Zhang, Q.; Li, Z. Investigation on the Explosion Limits and Flame Propagation Characteristics of Premixed Methanol-gasoline Blends. *Case Stud. Therm. Eng.* **2021**, *26*, 101000. [[CrossRef](#)]
38. Zhang, L.; Wang, H.; Chen, C.; Wang, P.; Xu, L. Experimental Study to Assess the Explosion Hazard of CH₄/coal Dust Mixtures Induced by High-temperature Source Surface. *Process Saf. Environ. Prot.* **2021**, *154*, 60–71. [[CrossRef](#)]
39. Li, L.; Liu, T.; Li, Z.; Chen, X.; Wang, L.; Feng, S. Different Prevention Effects of Ventilation Dilution on Methane Accumulation at High Temperature Zone in Coal Mine Goafs. *Energies* **2023**, *16*, 3168. [[CrossRef](#)]
40. Deng, L.; Lei, C.; Xiao, Y.; Cao, K.; Ma, L.; Wang, W.; Bin, L. Determination and Prediction on “three Zones” of Coal Spontaneous Combustion in a Gob of Fully Mechanized Caving Face. *Fuel* **2018**, *211*, 458–470. [[CrossRef](#)]
41. Ma, D.; Qin, B.; Gao, Y.; Jiang, J.; Feng, B. An Experimental Study on the Methane Migration Induced By Spontaneous Combustion of Coal in Longwall Gobs. *Process Saf. Environ. Prot.* **2021**, *147*, 292–299. [[CrossRef](#)]

Disclaimer/Publisher’s Note: The statements, opinions and data contained in all publications are solely those of the individual author(s) and contributor(s) and not of MDPI and/or the editor(s). MDPI and/or the editor(s) disclaim responsibility for any injury to people or property resulting from any ideas, methods, instructions or products referred to in the content.